



# Chronic UVA1 Irradiation of Human Dermal Fibroblasts: Persistence of DNA Damage and Validation of a Cell Cultured–Based Model of Photoaging

*Journal of Investigative Dermatology* (2019) **139**, 1821–1824; doi:10.1016/j.jid.2019.02.022

## TO THE EDITOR

Solar UVA, representing 90–95% of solar UV, can be subdivided into UVA2 (315–340 nm) and UVA1 (340–400 nm). UVA1 represents 75% of total solar UV and can induce reactive oxygen species (Tewari et al., 2012) and cyclobutane pyrimidine dimer (CPD) formation (Rochette et al., 2003). Penetration of UVR in human skin is wavelength-dependent and UVA1 penetrates into the deeper layers of the skin (D’Orazio et al., 2013). Exposure to UVA1 is exacerbated in indoor tanning users, where these rays are over-represented (Balk et al., 2013). UVA1 is less influenced than UVB by environmental and geo-orbital parameters (Marionnet et al., 2014), and are also the most difficult UV wavelengths to filter through sunscreens.

Many changes related to photoaging can occur in skin. Among them, the photoaging-induced changes in dermal extracellular matrix are well defined. They include the aberrant overproduction of elastin (Bernstein and Uitto, 1996) and a dysregulation of dermal collagens (Gniadecka et al., 1998). There is strong evidence showing that photoaging leads to a decrease in collagen synthesis (Quan et al., 2004). Moreover, UV-induced reactive oxygen species stimulate gene expression of collagen degrading matrix metalloproteinase (MMP) (Quan et al., 2009). These photoaging-related changes in the skin are primarily attributed to UVA wavelengths (Krutmann, 2000).

In this study, we have developed a photoaging model by chronically

irradiating fibroblasts with UVA1. We used residual CPDs, that we found both in the papillary dermis of sun-exposed skin and in chronically UVA1-exposed fibroblasts, as a marker of cumulative solar exposure. We used this model to determine transcriptomic changes that can occur in skin fibroblasts as a result of chronic UVA1 exposure.

All experiments performed in this study were conducted in accordance with our institution’s guidelines and the Declaration of Helsinki. The research protocols received approval by the Centre Hospitalier Universitaire de Québec institutional committee for the protection of human subjects with written informed patient consent.

## Residual CPDs in sun-exposed skin and chronically UVA1-irradiated dermal fibroblasts

We compared the accumulation of CPDs in human skin from breast reductions (unexposed) and facelifts (sun exposed) (Figure 1a, 1b), as well as in skin of dorsal (unexposed) and inner (sun exposed) forearm from nine individuals (Figure 1c, 1d). No CPD was detected in the epidermis, most likely due to damage dilution through the renewal of the epidermis. In dermis, where cells are non-dividing, we observed an accumulation of residual CPDs. This observation was possible in the most anterior, thus the most exposed to UVA, portion of the dermis, the papillary dermis. The observation of CPD accumulation in fibroblasts of the papillary dermis does not imply that they are absent in the reticular dermis, they are indeed difficult to quantify due

to the high autofluorescence of the collagen present in reticular dermis. UVB-induced CPDs in dermis is unlikely, due to UVB absorption in epidermis (Mallet et al., 2016; Tewari et al., 2012) and UVA induce CPDs preferentially in dermis (Tewari et al., 2012). Even if it cannot be excluded that some of the CPDs found in the papillary dermis are from UVB component of solar UV, these evidence strongly suggest that they are the result of exposure to the UVA component of solar UV.

UV-induced CPDs can be eliminated by DNA damage repair and dilution through DNA replication. We have shown that, in fibroblasts, the absence of repair in certain chromosomal regions results in chronic UVB-induced CPD accumulation (Berube et al., 2018). In vivo, the mitotic index of fibroblasts is very low in the dermis and declines with age (Gunin et al., 2011). The elimination of DNA damage through replicative dilution should therefore be minimal. We believe that CPDs found in fibroblasts of papillary dermis are the result of chronic UVA irradiation during life, coupled with a lack of repair in certain areas of the DNA.

We questioned the impact of residual UVA1-induced CPD on the functionality of dermal fibroblasts in connection with photoaging. To do so, we have developed an in cellulo photoaging model by chronically irradiating fibroblasts with 20 kJ/m<sup>2</sup> UVA1 (lamp spectrum in Supplementary Figure S1 online), two times a day, 4 days a week for 5 weeks. This chronic UVA irradiation protocol caused the accumulation of CPDs in fibroblasts (Figure 1e, 1f). This accumulation of CPDs is proportional to what is found in papillary dermis of exposed regions (Figure 1a–1d), suggesting that our

Abbreviations: CPD, cyclobutane pyrimidine dimer; MMP, matrix metalloproteinase

Accepted manuscript published online 13 March 2019; corrected proof published online 10 May 2019  
© 2019 The Authors. Published by Elsevier, Inc. on behalf of the Society for Investigative Dermatology.

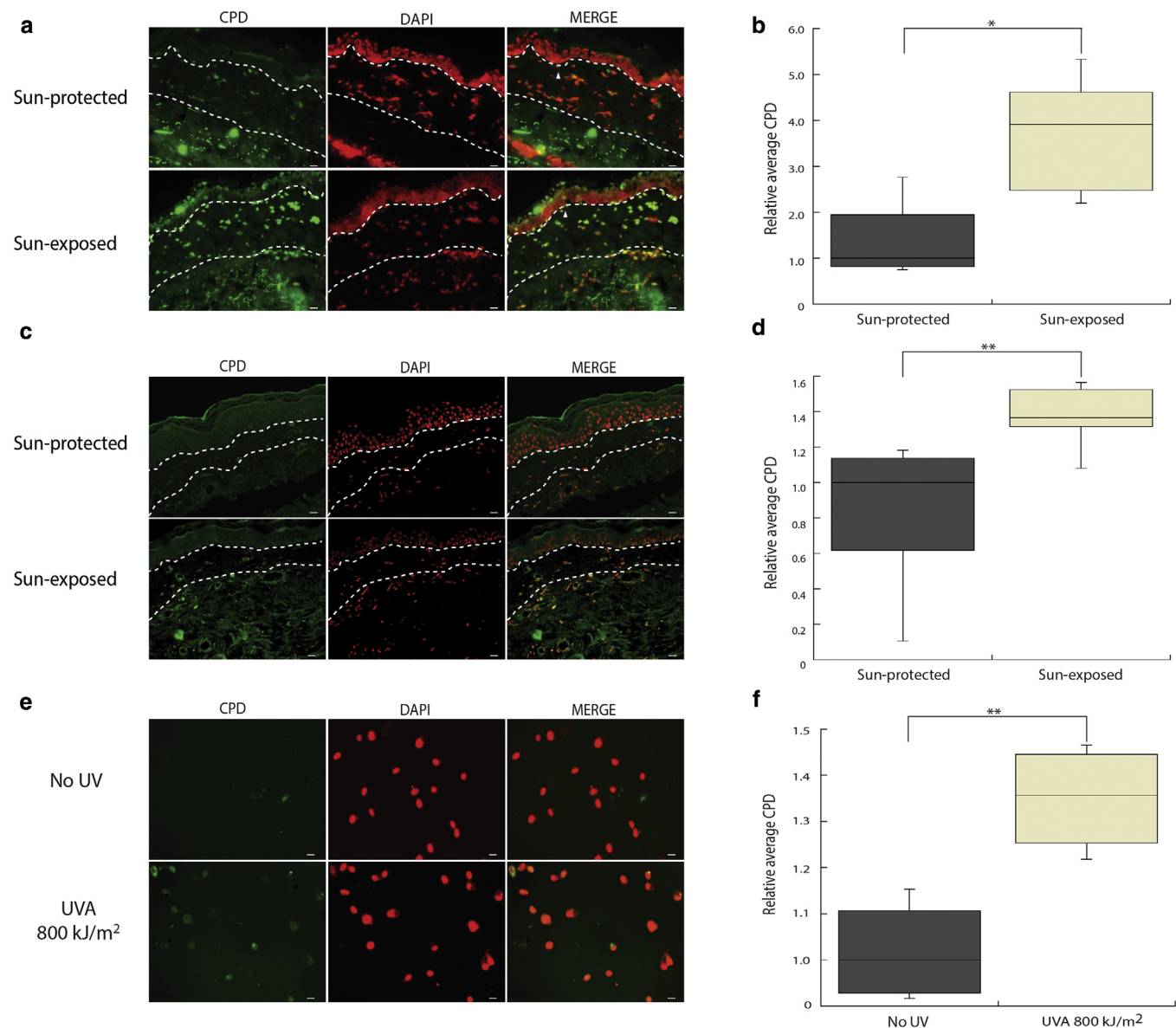


**Figure 1. Similar induction of residual CPDs in papillary dermis of sun-exposed skin and chronically UVA1-irradiated dermal fibroblasts.** Presence of CPDs was assessed in skin samples from (a) facelifts (sun-exposed;  $n = 6$ ) and breast reduction (unexposed;  $n = 4$ ), (c) dorsal (sun-exposed,  $n = 9$ ) and inner forearm (unexposed,  $n = 9$ ) from the same individual using anti-CPD antibody (green) and DAPI (red). Dotted lines delineate the papillary dermis. (b, d) Quantitative analysis of CPDs in papillary dermis shows significantly more residual CPDs in papillary dermis of sun-exposed skins. Data are presented as means  $\pm$  standard deviation.  $*P < 0.05$ ,  $**P < 0.005$ ; one-way analysis of variance for the paired samples (c, d) and Student  $t$  test for the unpaired samples (a, b). (e) The presence of CPDs in chronically UVA1-irradiated (UVA 800 kJ/m<sup>2</sup>) and unexposed fibroblasts (No UV) was detected using an anti-CPD antibody (green) and DAPI (red). (f) Quantitative analysis shows an accumulation of residual CPDs from the chronic irradiation similar to exposed papillary dermis. Data presented as means  $\pm$  standard deviation.  $P$ -value from one-way analysis of variance.  $n = 4$ . Scale bars = 20  $\mu$ m. CPD, cyclobutane pyrimidine dimer.

chronic UVA1 irradiation protocol mimics, at least in part, the cumulative solar exposure received by the dermis and can therefore be used as a model for skin photoaging. To our knowledge, this finding represents a previously unreported demonstration that chronic UVA1 irradiation can induce residual CPDs, and suggests that the residual CPDs found in the papillary dermis are the result of cumulative UVA exposure.

#### Gene-profiling analysis of extracellular matrix and MMP coding genes

We have then analyzed transcriptomic modifications related to the chronic UVA1 irradiation and consequently, to dermal photoaging (Supplementary Figure S2 online). Predominant collagens found in dermis (collagen I and III) have been found previously down-regulated in photoaging (Quan et al.,

2004). In this study, we have found that chronic UVA1 irradiation causes an important gene expression decrease of type I collagen by a factor of 1.8 to 6.5 (1A2 and 1A1, respectively) (Figure 2a, 2b) and of type III collagen (5.4-fold). These results are consistent with a phenotype of photoaging. Type V collagen, representing 5% of dermal collagen in vivo, has been found downregulated by 4.9 and 6.7 times

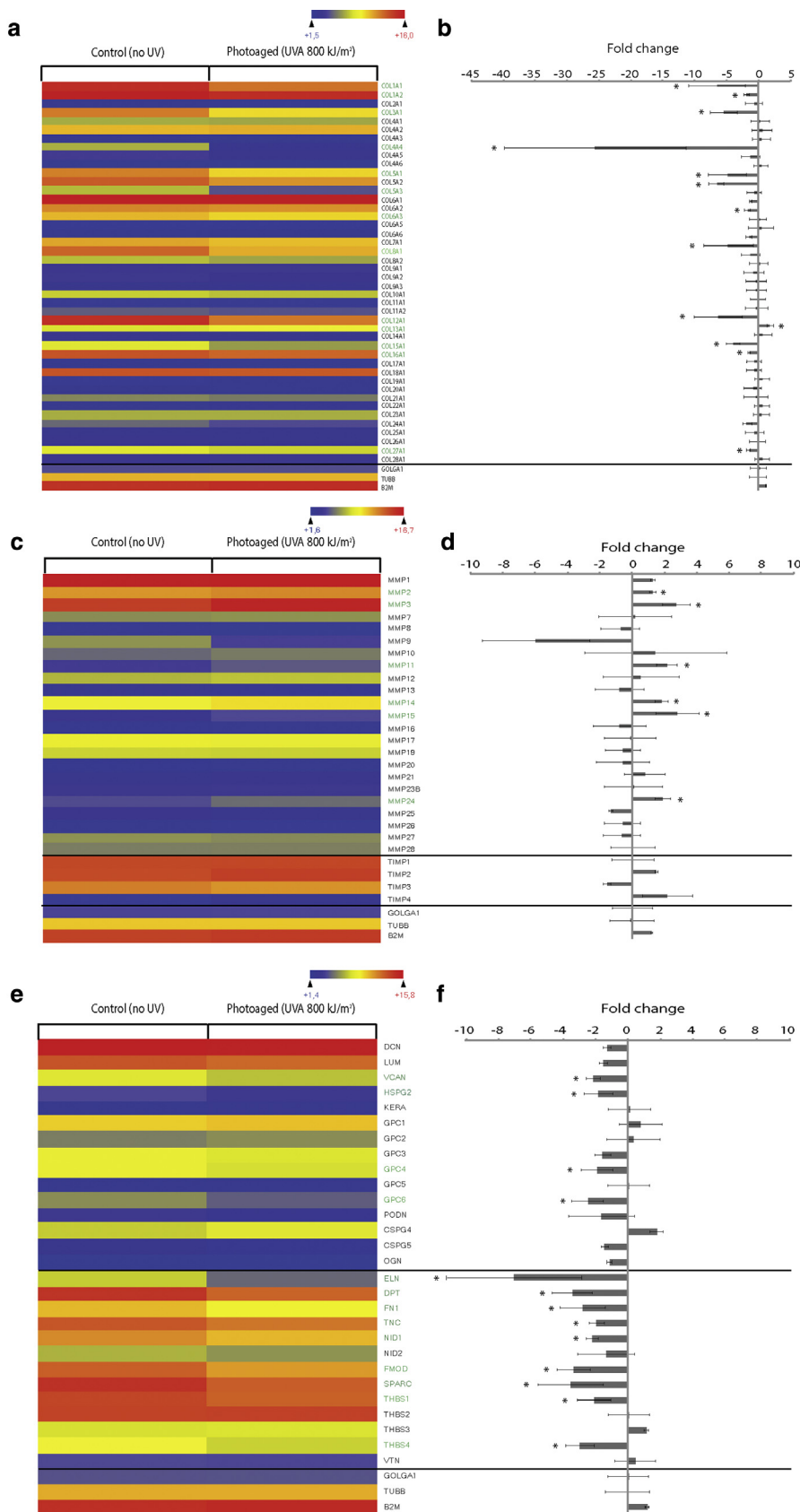


**Figure 2. UVA-induced extracellular matrix-related gene modification in human dermal fibroblasts.** Gene expression analysis of collagens (a, b), matrix metalloproteinase/tissue inhibitors of metalloproteinase (c, d), and other extracellular matrix components (e, f) in chronically UVA1-irradiated fibroblasts (UVA 800 kJ/m<sup>2</sup>) compared to unirradiated (No UV). Heatmap (a, c, e) and graphical

(5A1 and 5A3, respectively). We found a reduction of 25-fold of collagen 4A4, which is known as a major component of basement membrane. We find 28% of collagens (12/43), the expression of which is significantly reduced following chronic irradiation. Those results indicate that chronic UVA1 irradiation affects the capacity of fibroblasts to generate collagen.

#### MMP/tissue inhibitor of metalloproteinase

Overexpression of MMP1, 3, and 9 is associated to photoaging (reviewed in Quan et al., 2009). We observe non-significant variations of MMP1 and MMP9 gene expression, but a 2.8-fold increase in MMP3 expression level. This increase correlates with a photoaging phenotype following chronic UVA1 irradiation. Of all the MMPs analyzed, 26% are deregulated, all positively, following a chronic UVA1 irradiation. Tissue inhibitors of metalloproteinase, MMP antagonists, show no significant deregulation.

#### Proteoglycans and other extracellular matrix components

Versican, biglycan, and decorin are the three main proteoglycans found in the skin (reviewed in Lee et al., 2016). Our photoaging model shows a 2.1-fold decrease in versican expression, but no change in biglycan and decorin (Figure 2e, 2f), which correlates with previous observations made on photoaged skin (Lee et al., 2016). We observed a 6.9-fold reduction in the elastin gene expression level, which is in contradiction with the generally reported elastin increase following sunlight irradiation, but consistent with the previously

representation (b, d, f) of gene expression differences between irradiated and unirradiated fibroblasts. (a, b) Twelve collagen-coding genes are downregulated after chronic UVA1 irradiation, including genes from collagen I, III, IV, V, VIII, XII, XV, and XXVII families. (c, d) A general upregulation of matrix metalloproteinase-coding genes caused by UVA1 irradiation can be observed. Six matrix metalloproteinase-coding genes (matrix metalloproteinase 2, 3, 11, 14, 15, and 24) are upregulated. None of the tissue inhibitor of metalloproteinase is deregulated. (e, f) Four genes coding for proteoglycans are downregulated (VCAN, HSPG2, GPC4, and GPC6). Among other extracellular matrix-coding genes, ECN, DPT, FN1, TNC, NID1, FMOD, SPARC, THBS1, and THBS4 were downregulated.



observed decrease of elastin expression following a 1-week chronic UVA1 irradiation in fibroblasts (Zheng et al., 2018).

All those photoaging-related gene expression changes observed using narrow spectrum UVA1 highlight their importance in skin photoaging and the importance of extending the absorption spectrum of sunscreens formulas to wavelengths >340 nm via new ingredients or agents.

The data sets (microarray data) generated and analyzed during the current study are available in the Gene Expression Omnibus National Center for Biotechnology Information database for public access. The GSE accession number is GSE125429.

#### ORCIDiDs

Alicia Montoni: <http://orcid.org/0000-0002-8713-8103>

Kelly M. George: <http://orcid.org/0000-0001-5520-9897>

Jérémie Soeur: <http://orcid.org/0000-0001-6838-4299>

Christian Tran: <http://orcid.org/0000-0003-2244-3796>

Laurent Marrot: <http://orcid.org/0000-0001-5353-192X>

Patrick J. Rochette: <http://orcid.org/0000-0002-0678-8869>

#### CONFLICT OF INTEREST

KMG, JS, CT, and LM are employees of a company with a commercial interest in UV protection. AM and PJR state no conflict of interest.

#### ACKNOWLEDGMENTS

This work is supported by L'Oreal. PJR is a research scholar from the Fonds de Recherche du Québec, Santé.

#### AUTHOR CONTRIBUTIONS

Conceptualization: AM, KMG, JS, CT, LM, PJR. Data curation: AM, KMG, JS, CT, LM, PJR. Formal analysis: AM, CT, LM, PJR. Funding acquisition: KMG, JS, LM, PJR. Investigation: AM, KMG, JS,

CT, LM, PJR. Methodology: AM, CT. Project administration: KMG, LM, PJR. Resources: KMG, JS, CT, LM, PJR. Supervision: KMG, LM, PJR. Validation: AM, KMG, JS, CT, LM, PJR. Visualization: AM, KMG, LM, PJR. Writing—original draft: AM, PJR. Writing—review and editing: AM, KMG, JS, CT, LM, PJR.

**Alicia Montoni<sup>1</sup>, Kelly M. George<sup>2</sup>, Jérémie Soeur<sup>3</sup>, Christian Tran<sup>3</sup>, Laurent Marrot<sup>3</sup> and Patrick J. Rochette<sup>1,4,\*</sup>**

<sup>1</sup>Centre de Recherche du CHU de Québec-Université Laval, Axe Médecine Régénératrice, Hôpital du Saint-Sacrement, Québec, Canada;

<sup>2</sup>L'Oreal Research and Innovation, Clark, New Jersey, USA; <sup>3</sup>L'Oreal Research and Innovation, Aulnay sous Bois, France; and

<sup>4</sup>Université Laval, Faculté de Médecine, Département d'Ophtalmologie, Québec, Canada

\*Corresponding author e-mail: Patrick.rochette@orlo.ulaval.ca

#### SUPPLEMENTARY MATERIAL

Supplementary material is linked to the online version of the paper at [www.jidonline.org](http://www.jidonline.org), and at <https://doi.org/10.1016/j.jid.2019.02.022>.

#### REFERENCES

- Balk SJ, Fisher DE, Geller AC. Teens and indoor tanning: a cancer prevention opportunity for pediatricians. *Pediatrics* 2013;131:772–85.
- Bernstein EF, Uitto J. The effect of photodamage on dermal extracellular matrix. *Clin Dermatol* 1996;14:143–51.
- Berube R, Drigeard Desgarnier MC, Douki T, Lechasseur A, Rochette PJ. Persistence and tolerance of DNA damage induced by chronic UVB irradiation of the human genome. *J Invest Dermatol* 2018;138:405–12.
- D'Orazio J, Jarrett S, Amaro-Ortiz A, Scott T. UV radiation and the skin. *Int J Mol Sci* 2013;14:12222–48.
- Gniadecka M, Nielsen OF, Wessel S, Heidenheim M, Christensen DH, Wulf HC.

Water and protein structure in photoaged and chronically aged skin. *J Invest Dermatol* 1998;111:1129–33.

Gunin AG, Kornilova NK, Vasilieva OV, Petrov VV. Age-related changes in proliferation, the numbers of mast cells, eosinophils, and cd45-positive cells in human dermis. *J Gerontol A Biol Sci Med Sci* 2011;66:385–92.

Krutmman J. Ultraviolet A radiation-induced biological effects in human skin: relevance for photoaging and photodermatitis. *J Dermatol Sci* 2000;23(suppl 1):S22–6.

Lee DH, Oh JH, Chung JH. Glycosaminoglycan and proteoglycan in skin aging. *J Dermatol Sci* 2016;83:174–81.

Mallet JD, Dorr MM, Drigeard Desgarnier MC, Bastien N, Gendron SP, Rochette PJ. Faster DNA repair of ultraviolet-induced cyclobutane pyrimidine dimers and lower sensitivity to apoptosis in human corneal epithelial cells than in epidermal keratinocytes. *PLoS One* 2016;11:e0162212.

Marionnet C, Pierrard C, Golebiewski C, Bernerd F. Diversity of biological effects induced by longwave UVA rays (UVA1) in reconstructed skin. *PLoS One* 2014;9:e105263.

Quan T, He T, Kang S, Voorhees JJ, Fisher GJ. Solar ultraviolet irradiation reduces collagen in photoaged human skin by blocking transforming growth factor-beta type II receptor/Smad signaling. *Am J Pathol* 2004;165:741–51.

Quan T, Qin Z, Xia W, Shao Y, Voorhees JJ, Fisher GJ. Matrix-degrading metalloproteinases in photoaging. *J Invest Dermatol Symp Proc* 2009;14:20–4.

Rochette PJ, Therrien JP, Drouin R, Perdiz D, Bastien N, Drobetsky EA, et al. UVA-induced cyclobutane pyrimidine dimers form predominantly at thymine-thymine dipyrimidines and correlate with the mutation spectrum in rodent cells. *Nucleic Acids Res* 2003;31:2786–94.

Tewari A, Sarkany RP, Young AR. UVA1 induces cyclobutane pyrimidine dimers but not 6-4 photoproducts in human skin in vivo. *J Invest Dermatol* 2012;132:394–400.

Zheng Y, Xu Q, Chen H, Chen Q, Gong Z, Lai W. Transcriptome analysis of ultraviolet A-induced photoaging cells with deep sequencing. *J Dermatol* 2018;45:175–81.

## Expression Level of Prostaglandin D2 Receptor 2 Regulates Hair Regression

*Journal of Investigative Dermatology* (2019) 139, 1824–1828; doi:10.1016/j.jid.2019.02.012

#### TO THE EDITOR

Prostaglandin D2 (PGD2) is synthesized by the activation of prostaglandin D2 synthase (PTGDS), which can be regulated by androgens (Treister et al.,

2005; Zhu et al., 2004). PGD2 can also be nonenzymatically converted into 15-deoxy- $\Delta^{12,14}$ -prostaglandin J2 (15-dPGJ2). Both PGD2 and 15-dPGJ2 can bind to the prostaglandin D2

receptor 2 (DP2 receptor, also known as GPR44 and CRTH2). The expression levels of PGD2 and 15-dPGJ2 in balding scalps are higher than in non-balding scalps of men with male pattern baldness (Garza et al., 2012). Also, exogenous application of PGD2 hinders hair growth in mice and cultured human hair follicles, and this effect is lost in a DP2 receptor-knockout mouse (Garza et al., 2012;

Abbreviations: 15-dPGJ2, 15-deoxy- $\Delta^{12,14}$ -prostaglandin J2; DP, dermal papilla; DP2 receptor, prostaglandin D2 receptor 2; ORS, outer root sheath; PGD2, prostaglandin D2; PTGDS, prostaglandin D2 synthase; qPCR, quantitative PCR; siRNA, small interfering RNA

Accepted manuscript published online 27 February 2019; corrected proof published online 10 May 2019  
© 2019 The Authors. Published by Elsevier, Inc. on behalf of the Society for Investigative Dermatology.



## MATERIALS AND METHODS

All experiments performed in this study were conducted in accordance with our institution's guidelines and the Declaration of Helsinki. The research protocols received approval by the Centre Hospitalier Universitaire de Québec institutional committee for the protection of human subjects.

### Skin samples and cell culture

**Skin samples.** Two different series of skin samples were used in this project. (i) Skin from plastic surgery—breast reduction from four patients and facelift from six patients—were used as sun-protected and sun-exposed, respectively. The patients were all women, with a median age of 51 years old. Skin samples were collected within 1 hour post-surgery, embedded in water-based Tissue-Tek O.C.T. compound (Sakura, Torrance, CA) and kept at  $-80^{\circ}\text{C}$  until further analysis. Frozen tissues were cut in  $5\text{-}\mu\text{m}$  slices and mounted onto slides. (ii) Skin from a study conducted at the Clinical Research Center for Hair and Skin Science (Department of Dermatology and Allergy Charité-Universitätsmedizin, Berlin, Germany) from nine women aged between 55 and 75 years. In this study design, each subject was its own control: inner forearm was considered as a solar unexposed area, while dorsal forearm was considered as photo-exposed. Solar exposure prior to CPD assessment was carefully controlled in this study. Subjects were instructed to “completely avoid using sunbeds or sun exposure on the forearms and face within the 4 weeks before inclusion to the study and having planned UV sessions or sun exposure of the forearms and face during the study period.” Subjects were also instructed to “keep covered the investigational sites of biopsies until the last assessments (wear long armed clothes to protect the study site during the whole study.” Two-mm punch biopsies were performed on both inner and dorsal forearms. Skin samples were fixed with 10% phosphate buffered formaldehyde and embedded in paraffin. Section were cut in  $5\text{-}\mu\text{m}$  slices, mounted onto slides, de-waxed in xylene, and rehydrated in a graded ethanol series.

**Cell culture.** Normal human diploid fibroblasts were obtained by skin biopsy (mastectomy) and provided from four different healthy patients aged between 18 and 38 years. Cells were cultured in DMEM (cellgro; Corning, Tewksbury, MA)

complemented with 10% fetal bovine serum and 1% penicillin/streptomycin (Wisent, Saint-Jean-Baptiste, Quebec, Canada) at  $37^{\circ}\text{C}$ , 5%  $\text{CO}_2$ .

### UVA1 irradiation

Fully confluent fibroblasts were irradiated with a UVA1 lamp emitting UVA1 wavelengths (340–400 nm) with  $<0.01\%$  of UVA2 wavelengths (315–340 nm) (Supplementary Figure S1) (365-nm lamp with filter; UVP, Upland, CA) (Gendron and Rochette, 2015). Cells were irradiated with  $20\text{ kJ/m}^2$  UVA, two times a day, 4 days a week for 5 weeks ( $40 \times 20\text{ kJ/m}^2$ , for a total of  $800\text{ kJ/m}^2$  UVA). Each irradiation of  $20\text{ kJ/m}^2$  is the amount of UVA1 received by the skin in 25 minutes of exposure to the zenith sun (Kuluncsics et al., 1999). Those irradiation doses were used to avoid the death and senescence of the fibroblasts. We have not visually observed any cellular mortality or morphological changes that could be related to cell stress. Fibroblasts were brought to full confluency for at least 7 days before irradiation to prevent replication. During the irradiation, complemented DMEM medium was replaced by phosphate buffered saline (Wisent) to avoid oxidative stress coming from the irradiated culture medium components. New medium was added after each irradiation. For the control, cells from the same strain were cultured in the same conditions but were not UVA1-irradiated. The medium was changed to phosphate buffered saline at the same frequency as the irradiated cells.

### CPD detection

CPD detection has been performed on tissue from frozen and paraffin-embedded sections and on cultured cells using adapted protocols for each condition.

**OCT frozen sections.** CPD detection on frozen sections has been performed as described previously (Mallet et al., 2016; Mallet and Rochette, 2011, 2013). Briefly, slides were fixed in cold 70% ethanol and permeabilized in 0.3% Triton X-100 for 30 minutes at  $37^{\circ}\text{C}$ . RNase A treatment ( $100\text{ }\mu\text{g/ml}$  in Tris buffered saline [ $50\text{ mM}$  Tris-HCl, pH 7.6,  $150\text{ mM}$  NaCl]) was performed for 1 hour at  $37^{\circ}\text{C}$  before a denaturation in fresh  $0.07\text{ N}$  NaOH in 70% ethanol at room temperature for 2 minutes. Slides were dehydrated in a

graded ethanol series and air-dried before proteinase K treatment ( $10\text{ }\mu\text{g/ml}$  in  $20\text{ mM}$  Tris-HCl, pH 7.4,  $2\text{ mM}$   $\text{CaCl}_2$ ) 10 minutes at  $37^{\circ}\text{C}$ . After a 60-minute blocking in 5% BSA, 0.05% Tween-20 in Tris buffered saline, tissues were incubated overnight at  $4^{\circ}\text{C}$  in 1:2,500 mouse anti-CPD antibody (clone TDM-2; Cosmo Bio Co, Tokyo, Japan) followed by a 1-hour incubation in 1:2,500 fluorescein isothiocyanate-coupled goat anti-mouse antibody. Slides were counterstained with DAPI (1:2,000 in Tris buffered saline) and mounted with anti-fade solution.

**Paraffin-embedded sections.** The CPD immunostaining protocol was performed as described previously (Mitchell et al., 2001). Tissue samples were denatured in  $0.1\text{ N}$  NaOH in 70% ethanol for 15 minutes at room temperature, dehydrated in a graded ethanol series, and air-dried before proteinase K treatment ( $10\text{ }\mu\text{g/ml}$  in  $20\text{ mM}$  Tris-HCl, pH 7.4,  $2\text{ mM}$   $\text{CaCl}_2$ ) 10 minutes at  $37^{\circ}\text{C}$ . After a 30-minute blocking in 5% goat serum, slides were incubated overnight at  $4^{\circ}\text{C}$  in 1:1,000 mouse anti-CPD (clone TDM-2; Cosmo Bio Co) followed by a 1-hour incubation in 1:2,500 fluorescein isothiocyanate-coupled goat anti-mouse antibody. Slides were counterstained with DAPI (1:2,000 in Tris buffered saline) and mounted with anti-fade solution.

**Cells.** After chronic UVA1 irradiation of the four fibroblast strains, cells were harvested, counted, treated with 0.56% (weight/volume) KCl for 8 minutes at  $37^{\circ}\text{C}$ , fixed with Carnoy's solution (methanol:acetic acid, 3:1), and spread on glass slides as described previously (Rochette et al., 2005). The immunostaining protocol was performed as for frozen skin sections.

All specimens were observed with Zeiss Axio Imager.Z2 microscope equipped with Zeiss AxioCam MRm camera (Zeiss, Oberkochen, Germany). Signal quantification was done with the quantification module of AxioVision version 4.8.2 software (Zeiss).

At least three pictures of each sample were analyzed. In skin biopsies, the mean CPD (fluorescein isothiocyanate) signal in the papillary dermis of each picture was established for each sample. The mean  $\pm$  standard deviation of the samples was used for statistical analysis.

*P*-values were derived from a one-way analysis of variance test for the paired samples (sun-exposed and sun-protected from the same patient, Figure 1c, 1d)

and for the chronically irradiated cells (fibroblasts from the same patient irradiated or not, [Figure 1e, 1f](#)). *P*-values were derived from 2-tailed heteroscedastic Student *t* test for the unpaired samples (sun-exposed and sun-protected from different patients, [Figure 1a, 1b](#)).

### Gene profiling

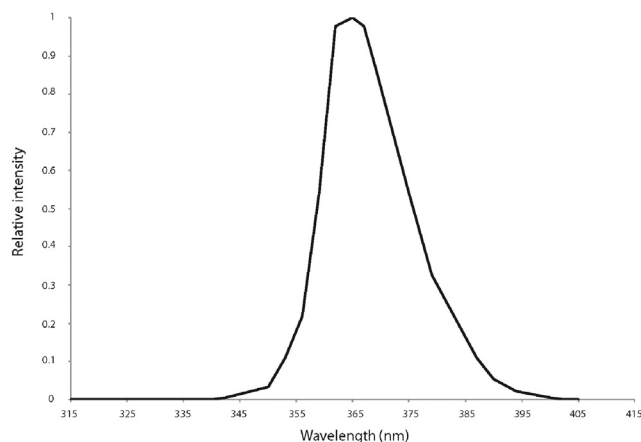
Gene expression analysis on microarray has been performed as published previously ([Gendron and Rochette, 2015](#)). Briefly, total RNA was isolated from the four strains of UVA1-irradiated and non-irradiated human diploid dermal fibroblasts at 100% confluency with TRIzol reagent (Ambion; Life Technologies, Carlsbad, CA) using the manufacturer's protocol. Cyanine 3-CTP (Agilent protocol)—labeled cRNA targets were prepared from 200 ng of total RNA from both experimental samples using the Agilent One-color Microarray-Based Gene Expression Analysis kit (Agilent Technologies, Santa Clara, CA). Then, 600 ng cRNA was incubated on a G4851A SurePrint G3 Human Ge 8 × 60 K array

slide (60,000 probes; Agilent Technologies). Slides were then hybridized for 18 hours, washed, and scanned on an Agilent SureScan Scanner. Data were then analyzed using the Arraystar V4.1 (DNAstar, Madison, WI) software for scatter plot and heatmap generation for selected genes. Statistical analysis of data has been performed using the robust multiarray analysis for background correction of the raw data values. Microarray data shown in this study comply with the MIAME (Minimum Information About a Microarray Experiment) requirements ([Brazma et al., 2001](#)).

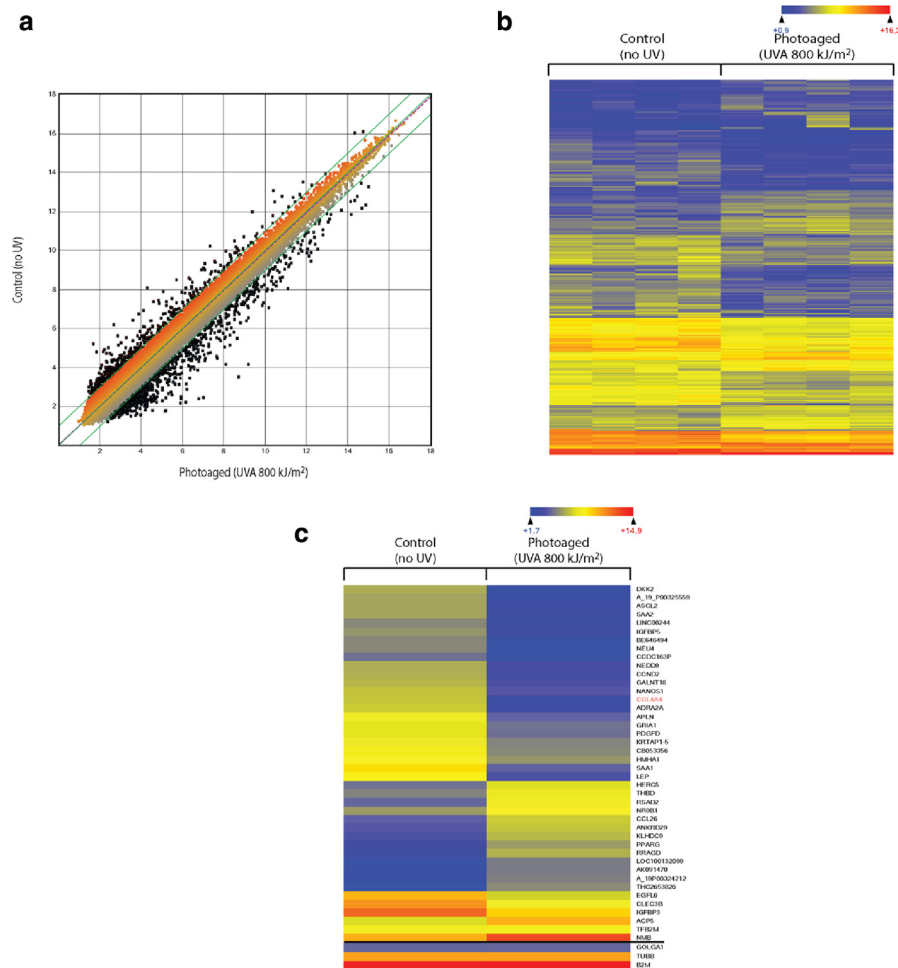
### SUPPLEMENTARY REFERENCES

- Brazma A, Hingamp P, Quackenbush J, Sherlock G, Spellman P, Stoeckert C, et al. Minimum information about a microarray experiment (MIAME)-toward standards for microarray data. *Nat Genet* 2001;29:365–71.
- Gendron SP, Rochette PJ. Modifications in stromal extracellular matrix of aged corneas can be induced by ultraviolet A irradiation. *Aging Cell* 2015;14:433–42.

- Kuluncsics Z, Perdiz D, Brulay E, Muel B, Sage E. Wavelength dependence of ultraviolet-induced DNA damage distribution: involvement of direct or indirect mechanisms and possible artefacts. *J Photochem Photobiol B Biol* 1999;49:71–80.
- Lee S, Jo M, Lee J, Koh SS, Kim S. Identification of novel universal housekeeping genes by statistical analysis of microarray data. *J Biochem Mol Biol* 2007;40:226–31.
- Mallet JD, Dorr MM, Drigeard Desgarnier MC, Bastien N, Gendron SP, Rochette PJ. Faster DNA repair of ultraviolet-induced cyclobutane pyrimidine dimers and lower sensitivity to apoptosis in human corneal epithelial cells than in epidermal keratinocytes. *PLoS One* 2016;11:e0162212.
- Mallet JD, Rochette PJ. Ultraviolet light-induced cyclobutane pyrimidine dimers in rabbit eyes. *Photochem Photobiol* 2011;87:1363–8.
- Mallet JD, Rochette PJ. Wavelength-dependent ultraviolet induction of cyclobutane pyrimidine dimers in the human cornea. *Photochem Photobiol Sci* 2013;12:1310–8.
- Mitchell DL, Meador JA, Byrom M, Walter RB. Resolution of UV-induced DNA damage in Xiphophorus fishes. *Mar Biotechnol* (NY) 2001;3(suppl 1):S61–71.
- Rochette PJ, Bastien N, Lavoie J, Guerin SL, Drouin R. SW480, a p53 double-mutant cell line retains proficiency for some p53 functions. *J Mol Biol* 2005;352:44–57.



**Supplementary Figure S1. Emission spectrum of the UVA1 lamp.** UVA1 irradiations were performed using B100 (UVP) lamps. The spectrum is derived from the manufacturer's specifications and modified according to the measurements made using an International Light double monochromator spectroradiometer (IL8000/760D/790).



**Supplementary Figure S2. Microarray analysis of UVA1-induced transcriptomic changes in human diploid dermal fibroblasts.** (a) Scatter plot of log2 signal intensity for 60,000 targets covering the entire human transcriptome. The signal for chronically UVA1-irradiated dermal fibroblasts (UVA 800 kJ/m²) (x-axis) is plotted against the signal of unirradiated fibroblasts (No UV) (y-axis). The >2-fold positively or negatively deregulated genes between the two conditions are represented by black dots. (b) Heatmap depicting the >2-fold positively or negatively deregulated genes in chronically UVA1-irradiated fibroblasts and unirradiated controls. The heatmap shows that the changes in gene expression caused by the chronic UVA1-irradiation are reproducible. The color scale used to display the log2 expression level values was determined by the hierarchical clustering algorithm of the Euclidian metric distance between genes. Genes indicated in dark blue correspond to those with an expression that is very low, whereas highly expressed genes are shown in orange/red.  $n = 4$ . (c) Heatmap depicting the most deregulated 42 genes by chronic UVA1 irradiation. Three control genes (GOLGA1, TUBB, and B2M) are used as experimental controls (bottom three genes of the heatmap). The transcription level of those genes is stable, independent of cell type and condition (Lee et al., 2007). Among the most deregulated genes, we find a 25-fold reduction in the gene encoding the  $\alpha$ -4 subunit of the type IV collagen (col4a1).